12TH CANADIAN CONFERENCE ON EARTHQUAKE ENGINEERING
JUNE 17-20, 2019
CHÂTEAU FRONTENAC
QUÉBEC, QC.
12ÈME CONFÉRENCE CANADIENNE DU GÉNIE PARASISMIQUE
17-20 JUIN 2019
CCEE 2019

Seismic Resistance of Tied GFRP-Reinforced Concrete Columns

Zahra Kharal[1], Shamim Sheikh[2]

[1] Postdoctoral Fellow, Department of Civil and Building Engineering, University of Toronto - Toronto, ON, Canada.
[2] Professor, Department of Civil and Building Engineering, University of Toronto - Toronto, ON, Canada.

ABSTRACT

A large inventory of deficient steel-reinforced concrete structures exists in which steel corrosion is the main cause of the deficiency. These structures are susceptible to collapse during a severe earthquake. Corrosion of steel in columns is especially a serious issue in existing structures. While upgrading of these structures is a priority, the new structures need to be built such that they don't undergo similar ageing problems. Research on glass fibre reinforced polymers, GFRP, as internal reinforcement has shown promise as a durable material for building sustainable infrastructure. The research reported here investigates the use of GFRP longitudinal bars and GFRP transverse reinforcement in columns for seismic resistance.

The experimental program involved testing of full-scale GFRP- and steel-RC columns under simulated earthquake loads. The variables investigated included column shape (circular or square), amount and spacing of transverse reinforcement, type of longitudinal and transverse reinforcement (steel or GFRP), reinforcement configuration and axial load level. The sections of the column specimens were 356 mm diameter, 500 mm diameter or 305 mm square. All the specimens were tested in a similar manner to provide directly comparable results to investigate the effects of the variables.

A significant conclusion drawn from this research is that GFRP spirals and ties can be used as primary transverse reinforcement in columns. They also confine the column concrete core more effectively than steel. GFRP longitudinal bars were found to resist about 60% of their tensile capacity in compression, but their low elastic modulus reduced the column capacity and stiffness.

In this paper, significant results and outcomes from a select group of specimens are presented. The relative performance of circular and square columns confined by lateral GFRP under seismic loading is evaluated. Additionally, the effectiveness of confinement provided by GFRP spirals in circular columns and GFRP rectilinear ties in square columns is discussed.

Keywords: Columns, GFRP, Seismic Loading, Confinement, Ties.

INTRODUCTION

Reinforced concrete (RC) columns are often the most critical elements in a structure. Yet, a large inventory of RC columns in North America contains inadequate lateral confinement in the potential plastic-hinge regions, requiring major seismic upgrade or retrofitting [1]. Moreover, the occurrence of corrosion is a huge issue in columns, which in conjunction with the already insufficient lateral steel, can lead to unexpected brittle structural failure during an earthquake or worse, under static gravity loads alone. Although, additional confinement can improve the seismic behaviour of these vulnerable columns, the process entails taking remedial measures after the column capacity has already been diminished as a result of steel corrosion. Glass fiber reinforced polymer (GFRP) bars due to their excellent corrosion resistance properties have been suggested as a pre-emptive measure for internal lateral reinforcement in new RC structures. However, GFRP cannot replace conventional steel on a one-to-one basis due to the significant differences in the mechanical properties of the two materials.

Recently, studies have reported that under concentric compression GFRP bars can be used as longitudinal reinforcement, and if designed properly, produce very robust columns [2, 3]. Lateral GFRP was found to be very effective in providing confinement, but replacing longitudinal steel bars with GFRP, irrespective of lateral reinforcement type (steel or GFRP), considerably reduced the column capacity. Although results from these studies provided valuable information, the loading pattern utilized did not reflect true column behaviour under realistic loads. A recent study on circular GFRP-RC column specimens confined by GFRP spirals tested under seismic loading displayed softer response and had lower energy capacity in comparison to comparable steel-RC columns [4]. There is a lack of similar studies on square columns confined by GFRP ties.

This lack of experimental data is one of the main reasons that the development of design code provisions on GFRP-RC columns is still lagging behind other components. For instance, the North American highway bridge codes (e.g. CAN/CSA-S6-14 [5]) have detailed design procedures for FRP-RC bridge decks, yet do not have any procedures for FRP-RC column design. Additionally, while there is a consensus among researchers that GFRP bars have a lower compressive strength than tensile strength, the decrease in compressive strength has been found to vary extensively, between 30% and 77% of the corresponding tensile strength [6, 7, and 8]. The scatter in data, in conjunction with the limited existing research on the subject, is partly the reason why major FRP design codes such as ACI-440.1R [9], CAN/CSA-S806 [10] and CAN/CSA-S6-14 [5] either do not recommend the usage of GFRP bars as longitudinal reinforcement in columns or neglect its compressive resistance.

EXPERIMENTAL PROGRAM AND RESTULTS

Specimen Details and Test Set-up

In one test series on square columns, a total of sixteen large-scale columns confined with GFRP ties were constructed and tested under seismic loading. While all the columns were confined by GFRP rectilinear ties, the longitudinal reinforcement type varied between the specimens, some specimens were reinforced with steel bars and others with GFRP. The specified concrete strength was 35 MPa for all columns. Due to the space limitation, only the results of four specimens will be discussed in this paper with a relevant comparison made with specimens from a previous study carried out on circular columns confined with GFRP spirals [11]; the geometry of these square and circular specimens is shown in Figure 1. The relevant details of these specimens can be seen in Table 1.

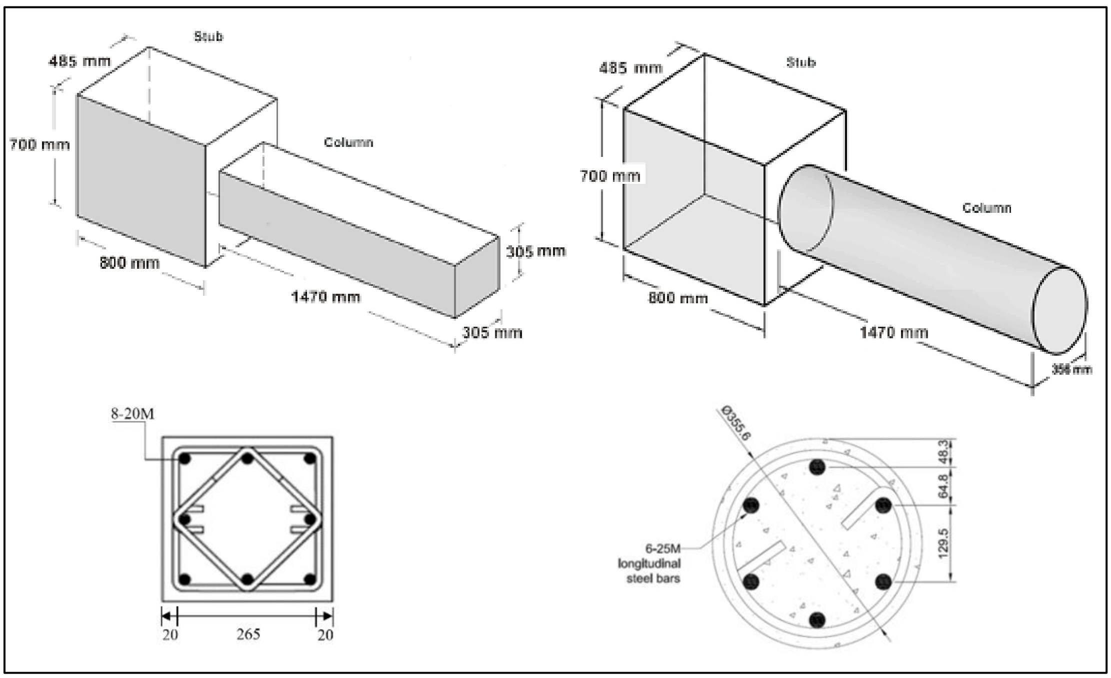

Figure 1 : Geometry of specimens: (a) circular, and (b) square

Table 1. Specimen Details.

Specimen Name	Concrete Strength	Specimen Shape	Longitudinal Bar Type	*GFRP Transverse Reinforcement*				Axial Load Level, $\frac{P}{P_o}$
				Bar Size	s (mm)	ρ_h (%)	f_u (MPa)	
TA-P28-S-6	42.4	Square	Steel	12	90	3.01	941	0.28
TA-P56-S-7	42.4		Steel	12	116	2.34	941	0.56
TA-P28-S-10	42.0		Steel	12	160	1.69	941	0.28
TA-P28-S-12	42.1		Steel	12	116	2.34	941	0.28
TA-P28-G-16	44.2		GFRP	12	90	3.01	941	0.28
P28-LS-12-50	40	Circular	Steel	12	50	3.00	914	0.28

Extensive instrumentation, namely LVDTs and strain gauges, were installed on all the specimens to gain a thorough understanding of the column behaviour. All the specimens were tested in the Column Testing Frame (CTF). The specimens were placed in the CTF in a horizontal position and subjected simultaneously to a pre-determined axial load and cyclic quasi-static lateral excursions simulating earthquake loading. Figure 2 shows the CTF test set-up with a fully instrumented specimen. The specimens were considered failed when they were unable to maintain the originally applied axial load.

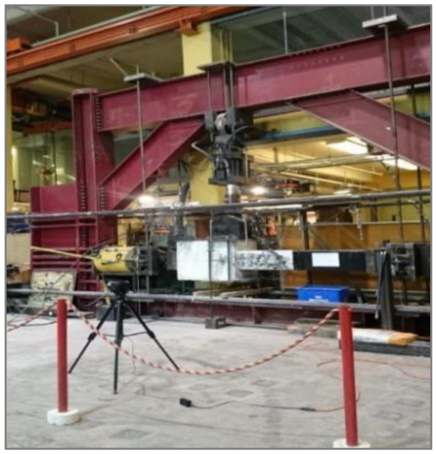

Figure 2 : Test Set-up

GFRP Coupon Tests

Tensile properties of straight GFRP bars made from the same batch as the GFRP ties were determined as per the requirements of ASTM D7205 [12]; the tensile strength f_u values have been provided in Table 1. The typical failure mode of these tensile coupons can be seen in Figure 3a. In addition to the tensile properties, the behaviour of the GFRP bars used as longitudinal reinforcement in the columns was also determined since the mechanical properties of GFRP bars in tension and compression can differ significantly, unlike steel. The ASTM 0695 [13] standard was found to be inadequate to accurately assess the compression strength of GFRP bars by researchers [8]. For consistency with similar previous studies on circular columns, the procedure utilized by Tavassoli et al. [4] to determine the properties of GFRP bare bars in compression was adopted. The free length of the specimens corresponded to the spacing of the ties in the column specimens. The typical failure mode was mainly due to the crushing of fibres, as shown in Figure 3b. The modulus of elasticity determined from the compression coupon test were similar to the values obtained from the tensile coupon tests. On the other hand, the ultimate compressive failure strengths was observed to be slightly larger than 60% of the corresponding tensile strength values for the unsupported lengths of bars in the columns.

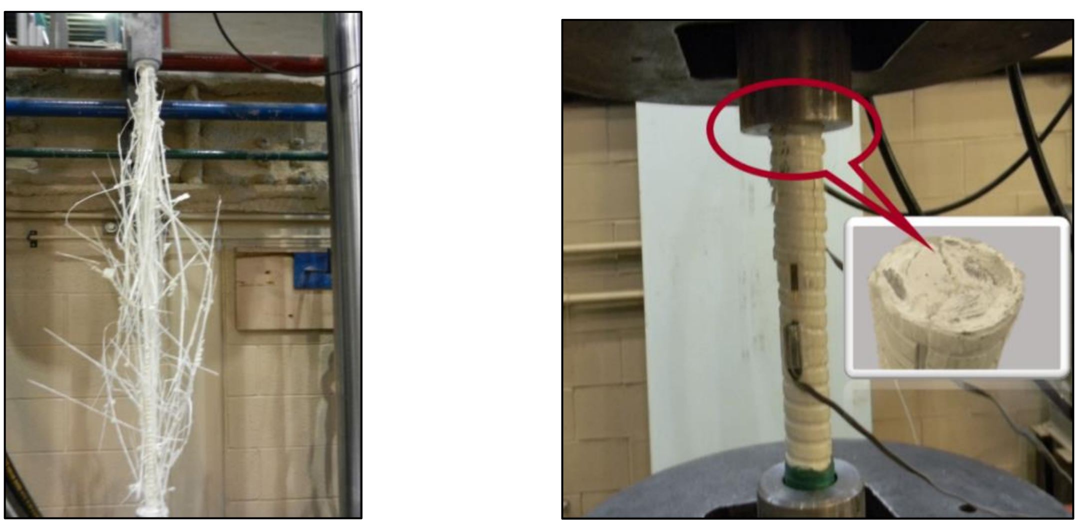

(a) *(b)*

Figure 3. Failure Modes of the GFRP Coupons in: (a) tension, and (b) compression.

Column Test Results

The performance of the specimens for seismic behavior was mainly evaluated by plotting the hysteresis responses in terms of lateral shear vs. tip deflection (*V–Δ)* and moment vs. curvature (*M–ϕ)* and calculating the ductility parameters. In this section, the effects four variables, namely axial load level, amount of GFRP lateral reinforcement, longitudinal bar type and GFRP spiral vs ties, are discussed by comparing the envelope *V–Δ* and *M–ϕ* curves. The envelope curves were normalized with respect to nominal capacities, V_n or M_n, to minimize the effect of any variation which exists between the specimens' concrete strengths.

1. *Axial Load*

The effect of axial load level on the performance of square specimens confined by GFRP ties is evaluated by comparing the results of specimens TA-P28-S-12 and TA-P56-S-7, subjected to axial load levels of $0.28P_o$ and $0.56P_o$, respectively. The specimens were almost identical in every other aspect. The normalized *V–Δ* and *M–ϕ* envelope curves of the two column specimens, compared in Figure 4, clearly show that an increase in the axial load level resulted in a considerable decrease in ductility; the behaviour of specimen TA-P56-S-7 subjected to $0.56P_o$ can be clearly seen to be considerably less ductile than its companion specimen, showing an early higher strength followed by a rapid strength deterioration before failure. Axial load level can be seen to affect the sectional behaviour (*M–ϕ*) considerably more than the member behaviour (*V–Δ)*. This behaviour was similar to the effect of axial load level that has been observed in conventional steel reinforced columns and external FRP confined columns [1, 14].

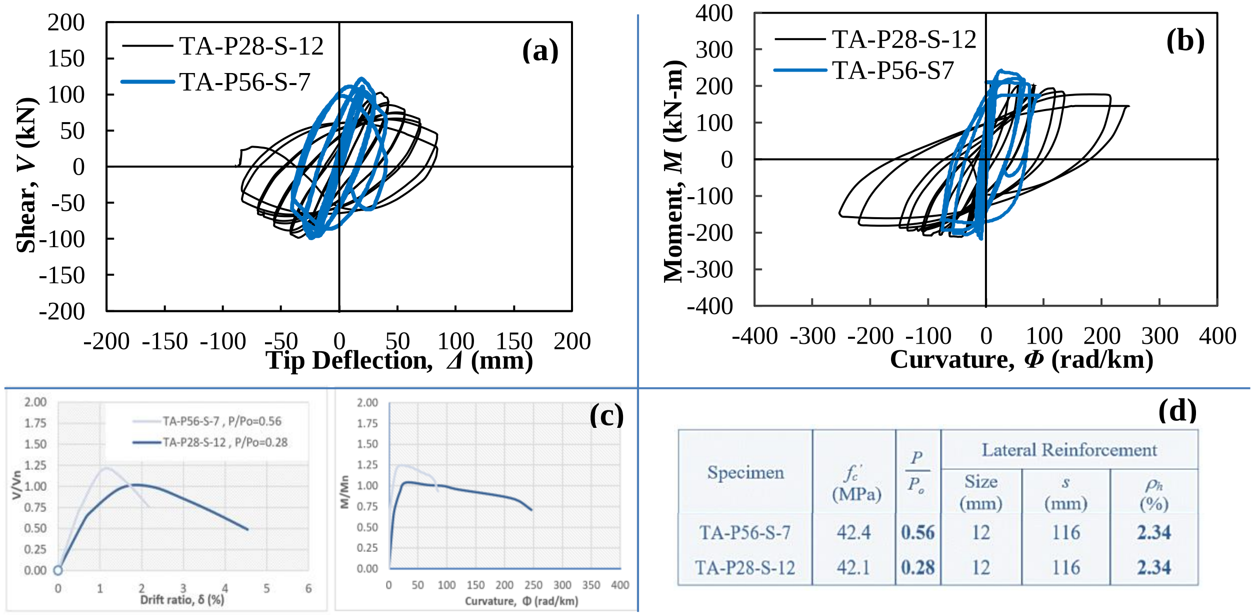

Specimen	f_c' (MPa)	$\frac{P}{P_o}$	Lateral Reinforcement Size (mm)	Lateral Reinforcement s (mm)	Lateral Reinforcement ρ_h (%)
TA-P56-S-7	42.4	**0.56**	12	116	**2.34**
TA-P28-S-12	42.1	**0.28**	12	116	**2.34**

Figure 4. Effect of Axial Load Level: (a) V–δ hysteresis response, (b) M–ϕ hysteresis response, (c) envelope curves, and (d) specimen details

2. *Amount of Reinforcement*

An increase in GFRP lateral reinforcement ρ_h resulted in an improvement in the overall column behavior as can be seen in Figure 5 from the results of specimen TA-P28-S-6 and TA-P28-S-10; the former specimen had a reinforcement ratio ρ_h of 3.01% and the latter 1.69%, respectively. TA-P28-S-6 underwent fifteen lateral displacement cycles before failure compared to ten for TA-P28-S-10. An increase from 1.69% to 3.01% in ρ_h resulted in specimen 6 achieving a tip displacement of almost 100 mm (6.76% drift ratio) in comparison to the tip displacement of 70 mm (3.80% drift ratio) for TA-P28-S-10.

The direct comparison between the *M–ϕ* envelope curves of the two specimens in Figure 5 shows that specimen TA-P28-S-10 experienced a much more rapid decrease in moment post-peak. In addition to an improvement in curvature, an increase in flexural strength was also observed in the response of TA-P28-S-6. The *V–δ* envelope response of the two specimens indicates that an increase in ρ_h had a favourable effect on drift capacity as well, but the improvement in member behaviour was considerably less than the sectional behaviour. Additionally, no significant effect was observed on the shear load of the specimens.

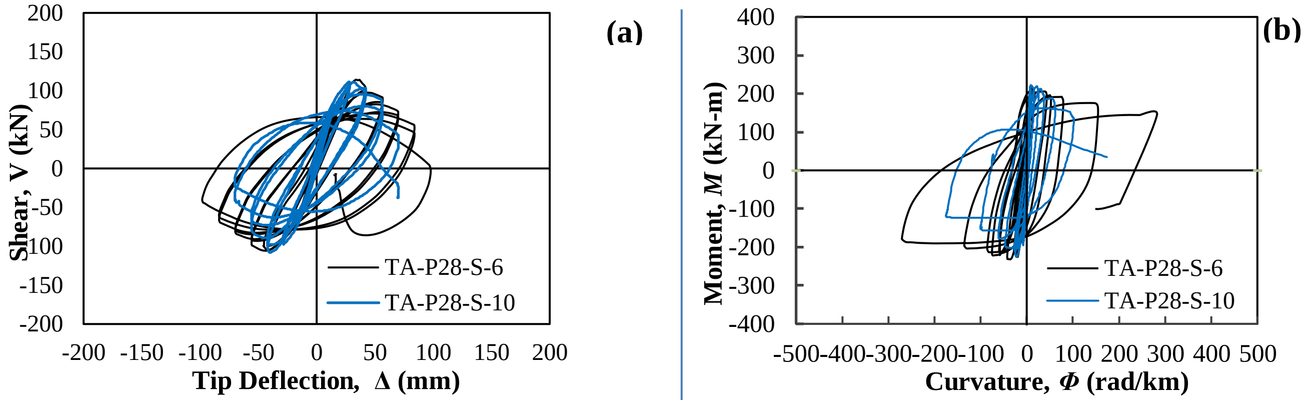

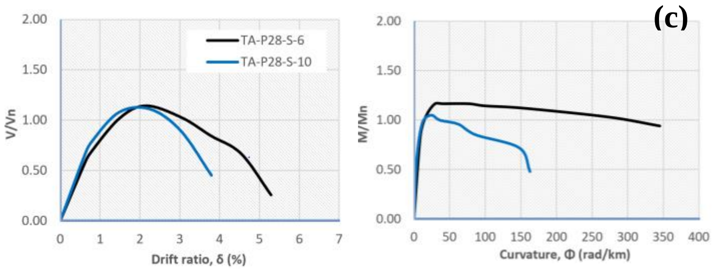

(d)

Specimen	f_c' (MPa)	$\frac{P}{P_o}$	Lateral Reinforcement Size (mm)	Lateral Reinforcement s (mm)	Lateral Reinforcement ρ_h (%)
TA-P28-S-6	42.4	0.28	12	90	**3.01**
TA-P28-S-10	42.0	0.28	12	160	**1.69**

Figure 5. Effect of amount of lateral reinforcement: (a) V–δ hysteresis response, (b) M–ϕ hysteresis response, (c) envelope curves, and (d) specimen details

3. *Longitudinal Bar Type*

The failure mode of column specimen TA-P28-G-16 with GFRP longitudinal bars differed significantly from its comparable specimen with steel longitudinal bars, specimen TA-P28-S-6. Specimens TA-P28-S-6 and TA-P28-G-16 were identical in all aspects, except that the former was reinforced with 8-20 M steel longitudinal bars and the latter with 8-20 mm GFRP longitudinal bars. However, unlike specimen TA-P28-S-6, in which the primary mode of failure was due to the failure of GFRP ties, the mode of failure in specimen TA-P28-G-16 was due to the crushing of GFRP longitudinal bars; this crushing is shown in Figure 6. The compressive strength of the GFRP longitudinal bars was determined by monitoring the strain in the bars. At failure, on the compression side, the calculated compressive stress in the GFRP longitudinal bars for specimen 16 was approximately 696 MPa, about 61% of the ultimate tensile strength. This showed that the compressive strength of GFRP bars obtained under seismic loading correlates very well with the strength obtained via coupon tests.

Figure 6. Crushing of GFRP longitudinal bar in Specimen 16

Figure 7 compares the *V–Δ* and *M–ϕ* envelope curves of the two specimens. The low stiffness of GFRP longitudinal bars in specimen TA-P28-S-6 resulted in a 27% lower flexural capacity and 30% lower shear capacity. In the *V–Δ* relationship shown in Figure 7, specimen TA-P28-G-16 can be seen to have a longer post-peak descending branch than specimen TA-P28-S-6 resulting in a noticeably larger deflection. Specimen TA-P28-G-16 also resisted 10 additional load cycles than specimen TA-P28-S-6. This can be attributed to the fact that once steel longitudinal bars yield, the tangent modulus is almost negligible, resulting in a higher susceptibility to $P\Delta$ effect and buckling under compression while GFRP longitudinal bars have constant stiffness until failure, and thus display more stable behaviour at high strains. The moment capacity of specimen TA-P28-S-6 was observed to gradually decrease after the peak moment, which occurred close to the steel yield, while the moment capacity of specimen TA-P28-G-16 increased at an almost constant rate until failure.

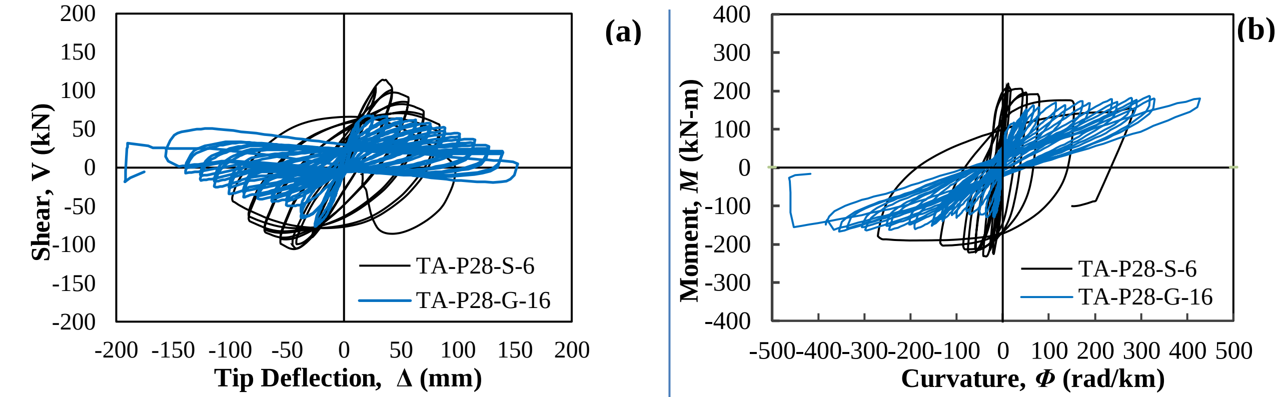

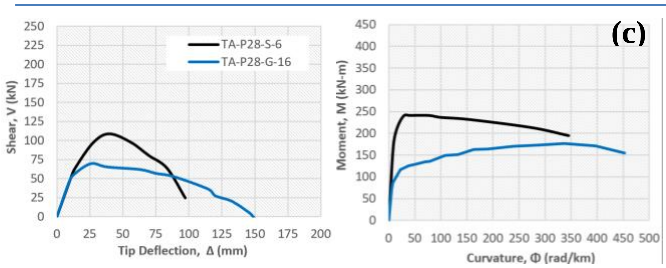

(d)

Specimen	f_c' (MPa)	$\frac{P}{P_o}$	Lateral Reinforcement			Longitudinal Bar Type
			Size (mm)	s (mm)	ρ_{sh} (%)	
TA-P28-S-6	43.5	0.28	12	123	2.34	**Steel**
TA-P28-G-16	45.3	0.28	12	68	2.34	**GFRP**

Figure 7. Effect of Longitudinal Bar Type: (a) V–δ hysteresis response, (b) M–ϕ hysteresis response, (c) envelope curves, and (d) specimen details

4. *GFRP Ties versus GFRP Spirals*

The results of the square specimen TA-P28-S-6 were compared to those of specimen P28-LS-12-50, a circular column with steel longitudinal bars and GFRP spirals tested by Tavassoli and Sheikh [11]. The spacing of the transverse reinforcement of the square and circular columns were 90 mm and 50 mm, respectively, resulting in almost the same lateral reinforcement ratio ρ_h of about 3.0%; the columns were almost identical in every other aspect. In the circular column, no redundancy was observed after the rupture of GFRP spirals and thus the confinement provided to the core concrete diminished as soon as the spirals ruptured [11]. The loss of confinement in the square column was found to be not quite as sudden; the failure was more prolonged since there were two ties at each level, and it took several cycles for both the ties to fail. The failure mode for both specimens is shown in Figure 8.

Figure 8. Effect of Longitudinal Bar Type on V–Δ and M–ϕ Response

Figure 9 shows the V-δ and M-ϕ normalized envelope curves, respectively, of the square column TA-P28-S-6 and circular column P28-LS-12-50. The behaviour of the circular column confined by GFRP spirals was clearly superior to the square column confined by GFRP rectilinear ties partly due to smaller spacing of transverse reinforcement. Specimen P28-LS-12-50 endured 21 lateral cycles before failure compared to the 15 cycles of TA-P28-S-6. The flexural strength enhancement M/M_n improved as a direct result of the change in column section, from 1.16 for the square section to 1.21 for the circular section. Additionally, it was observed that the circular column had more or less constant moment until failure whereas the square column experienced a descending post-peak branch of M-ϕ envelope. This makes sense since unlike circular columns, the concrete core in the square column was not fully and uniformly confined by perimeter ties.

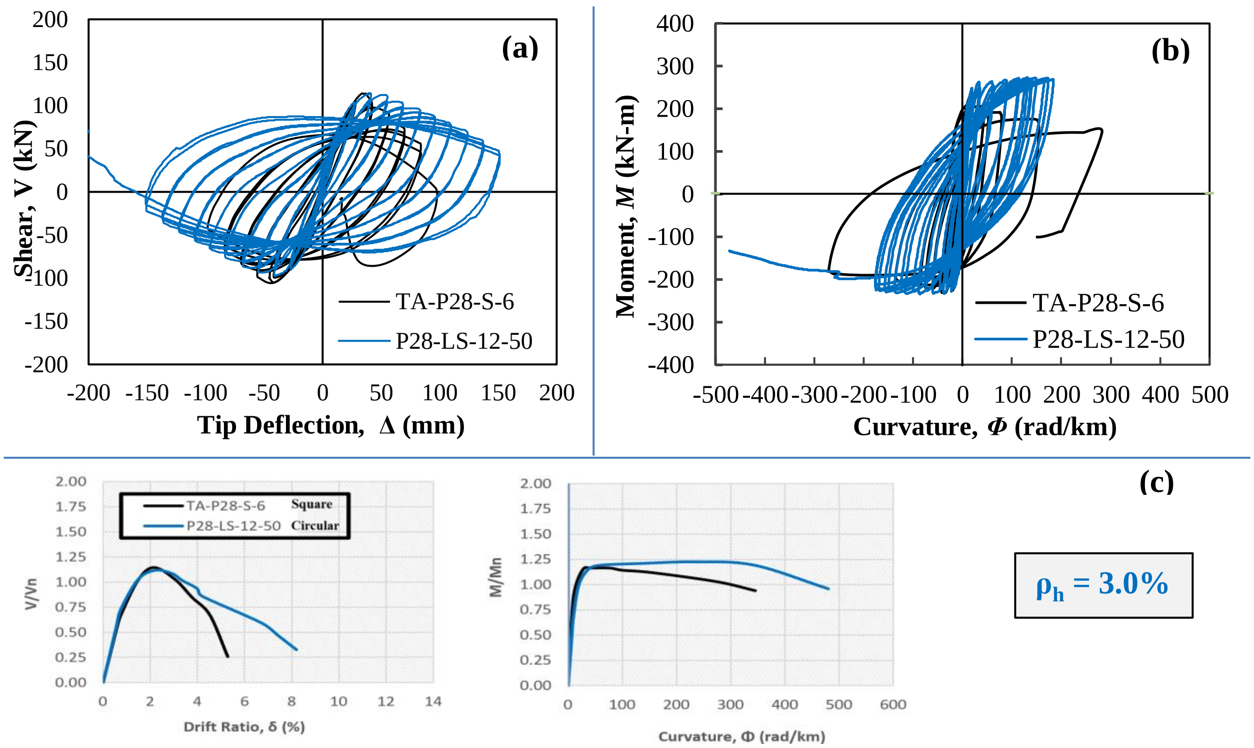

Figure 9. Effect of Section Geometry: (a) V–δ hysteresis response, (b) M–ϕ hysteresis response, and (c) envelope curves

CONCLUSIONS

This study investigated the application of corrosion-resistant GFRP ties in square columns under constant axial load and cyclic lateral displacement excursions simulating earthquake forces. The behaviour of the columns was studied based on physical observations, and the moment-curvature and shear-deflection envelope responses. Comparisons of the specimen responses were made within this study and with previous comparable studies to highlight the effects of different variables on the column performance. A few of the main conclusions related to column responses are listed below:

- GFRP rectilinear ties can be used as primary lateral reinforcement for shear and confinement in concrete columns designed for seismic resistance. GFRP lateral reinforcement provides continuous confinement to the columns resulting in large deformability and ductility values.

- The columns with GFRP ties and GFRP longitudinal bars displayed stable column behaviour and were able to undergo a large number of cycles and achieve high deformability levels before failure. The flexural strength and stiffness of these columns were found to be lacking in comparison to the columns with steel longitudinal bars and GFRP ties.

- The modulus of elasticity of the GFRP longitudinal bars in compression was found to be similar to that obtained from tensile tests while the ultimate compressive failure strength was observed to be about 60% of the corresponding tensile strength values.

- The behaviour of circular columns confined with GFRP spirals was clearly superior to square columns confined with GFRP ties. However, it was observed that for circular columns, there was no redundancy after the rupture of GFRP spiral and confinement provided to the core concrete diminished as soon as the spirals ruptured. In square columns, the failure was more prolonged since there were two ties at each level, and it took several cycles for the ties to unhook and they did not give away suddenly.

• In square columns, the optimum solution with respect to strength, stiffness, ductility, energy dissipation, and corrosion resistance, thus, appears to be a hybrid column with steel longitudinal bars and GFRP transverse reinforcement.

ACKNOWLEDGMENTS

The financial support of Natural Science and Engineering Research Council (NSERC) of Canada, Ontario Graduate Scholarship (OGS) program, and India-Canada Centre for Innovative Multidisciplinary Partnerships to Accelerate Community Transformation and Sustainability (IC-IMPACTs), an NSERC network of centre of excellence, are greatly appreciated. The author would like to acknowledge Fiberline Composites and Schöck Canada for providing the FRP materials. Special thanks are due to Schöck Germany for their help in the design and manufacturing of the special ties for the column specimens. Dufferin Concrete generously donated the concrete for this experimental program. The experimental work reported here was carried out in the Structures Laboratories of the University of Toronto.

REFERENCES

[1] FHWA-RD-98-088. (1998). “Corrosion protection: Concrete bridges.” De Luca, A., Matta, F., and Nanni, A. (2010). “Behavior of full-scale glass fiber-reinforced polymer reinforced concrete columns under axial load.” ACI Struct. J., 107(5), 589–596.

[2] Affifi, M.Z., Mohamed, M.H., and Benmokrane, B. (2013). “Axial Capacity of Circular Concrete Columns Reinforced with GFRP Bars and Spirals” J. Compos. Constr., 10.1061/(ASCE)CC.1943-5614.0000438.

[3] Tavassoli, A., Liu, J. and Sheikh, S. (2015). “Glass fiber-reinforced polymer-reinforced circular columns under simulated seismic loads.” ACI Struct. J., 112(10), 103–114.

[4] CSA (Canadian Standards Association) (2014). “Canadian Highway Bridge Design Code.” CAN/CSA-S6-14, Rexdale, Ontario, Canada, 788.

[5] Kobayashi, K., and Fujisaki, T. (1995). “Compressive Behavior of FRP Reinforcement in Non-Prestressed Concrete Members,” Proceedings of the 2nd International RILEM Symposium on Non-Metallic (FRP) Reinforcement for Concrete Structures, Ghent, Belgium, pp. 267-274.

[6] Deitz, D. H.; Harik, I. E.; and Gesund, H. (2003). “Physical Properties of Glass Fiber Reinforced Polymer Rebars in Compression.” Journal of Composites for Construction, V. 7, No. 4, pp. 363-366.

[7] Bruun, E. and Sheikh, S. A. (2014). “GFRP Bars as Compressive Reinforcement in Exposed Structures”, 9th International Conference on Short and Medium Span Bridges, Calgary, Alberta, Canada, July 15-18, 2014.

[8] ACI (American Concrete Institute). (2015). “Guide for the design and construction of structural concrete reinforced with fiber-reinforced polymer (FRP) bars.” ACI 440.1R-15, Farmington Hills, MI.

[9] CSA (Canadian Standards Association). (2012). “Design and construction of building components with fibre-reinforced polymers.” CSA S806-12, Rexdale, ON, Canada, 177.

[10] Tavassoli, A., and Sheikh, S.A. (2017). “Seismic Resistance of Circular Columns Reinforced with Steel and GFRP.” ASCE Journal of Composites for Construction, Jan. 23, 2017. DOI: 10.1061/(ASCE) CC.1943-5614.0000774

[11] ASTM. (2016). “Standard test method for tensile properties of fiber reinforced polymer matrix composite bars.” ASTM D7205/D7205M–16, West Conshohocken, PA.

[12] ASTM. (1990). “Standard Test Method for Compressive Strength of Carbon and Graphite.” ASTM C695-1990, ASTM International, West Conshohocken, PA.

[13] Sheikh, S. A., and Khoury, S. S. (1993). “Confined concrete columns with stubs.” ACI Struct. J., 90(4), 414–431.